#25-020
2025 AFS Proceedings ©American Foundry Society

Bio-based Foam Patterns for Lost Foam Casting

Jacob Belke,[1] Adam Kopper,[1] Tedd Sheets,[2] Dan Mueller,[3] Sam Bhargava,[4]
Chris Mercy,[4] Jonathan Godfrey[4]

[1]Mercury Marine, Fond du Lac, Wisconsin, USA
[2]Betz Industries, Grand Rapids, Michigan, USA
[3]ATLAS Molded Products, Fond du Lac, Wisconsin, USA
[4]Lifoam Industries LLC, Greer, South Carolina, USA

ABSTRACT

The lost foam casting process has used expanded polystyrene (EPS) as the pattern material since the inception of the process. The expanded polystyrene is derived from petroleum distillation which carries a heavy carbon footprint and health concerns from the decomposition products during casting. A novel molding bead technology has emerged that derives an expandable polylactic acid (EPLA) foam molding bead from sustainable domestic biological sources. Bio-based foam patterns were evaluated for their potential to replace EPS as a lost foam pattern material using laboratory testing and casting trials. The lab results showed the EPLA materials did not produce hazardous air pollutants (HAPs) nor carcinogens. The casting trials successfully produced lost foam castings in both aluminum and gray cast iron without any modifications to the lost foam casting process.

Keywords: lost foam, polystyrene, bio-foam, PLA, sustainability, aluminum, cast iron

INTRODUCTION

The lost foam casting process utilizes expendable polymeric patterns produced using expanded polystyrene (EPS). Polystyrene (PS) is a polymer of styrene (C_8H_8) which is a product of the fractional distillation of crude oil, more specifically the alkylation of benzene with ethylene. Ferrous casters typically use a mixture of PS and polymethylmethacrylate (PMMA) to slow the metal front during filling, reducing the potential for fold defects. For EPS, the PS beads are impregnated with a hydrocarbon, typically n-pentane, which allows the PS beads to expand during molding. After molding, the concentration of hydrocarbons inside the beads is negligible as the gas diffuses out of the PS.

Petroleum refineries are generally considered a major source of hazardous and toxic pollutants (air, land, water).[1,2] Additionally, crude oil is classified as a non-renewable resource as the resource is used faster than it naturally replenishes meaning the worlds crude oil supply is finite.[3] In 2016, there was an estimated 1.65 trillion barrels of oil reserves left in world, which at our current rate of consumption equates to 47 years[4,5] However, with new legislation and increasing governmental emission restrictions globally, the end date of crude oil production could be well before the global oil reserves are exhausted. The lost foam casting process likely would not survive to the end of the oil industry as the world economy is based on capitalism. As the supply of petroleum decreases, the cost of lost foam will increase to the point of being priced out of the casting market.

The lost foam casting processes are considered relatively energy efficient (~27% less than green sand[6]) with minimal waste compared to other sand-casting processes. As with other metalcasting processes, emissions of particulates, metallic oxide fumes, and hazardous air pollutants (HAPs) are a concern in lost foam.[7] During casting, polystyrene decomposes into benzene, ethyl benzene, styrene, toluene, and other light hydrocarbon species (Figure 1) where PMMA decomposes solely into light carbon components. Some decomposition products (polynuclear aromatic compounds, anthracene, naphthalene, phenanthrene, benzofluoranthene, and benzopyrene) have been found to be carcinogenic.[7]

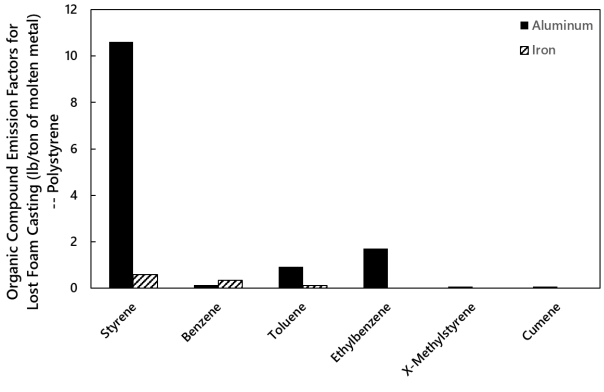

Figure 1. Total amounts of decomposition products of polystyrene measured from aluminum and iron casting processes.[8]

The lost foam casting process can trace its history back to the original 1956 patent for an evaporative-pattern casting process by Harold Shroyer. In Shroyer's patent, polystyrene is repeatedly listed to be the inexpensive expanded plastic of choice for patterns with only one mention of polyethylene as an alternative.[9] It is later explained that polystyrene was the only material tested as a pattern material and thus was used for the process. Guler et al. briefly experimented with expanded polyethylene (EPE) and found that it is possible to use EPE for the lost foam casting process if the right parameters are used.[10] Unfortunately, the parameters used in the experiment were not properly specified to represent what would be done commercially.

Polymers derived from biological sources have been successfully produced and are becoming ever cheaper and more accessible. In the last couple decades, polymers have been developed from biologically sourced materials including starch, cellulose, fatty acids, sugars, proteins, and other sources. Polymers resulting from these sources (Table 1) have not been previously explored for use as lost foam patterns except for polyethylene (PE).[10]

Table 1. Bioplastics and their Bio-derived Monomer

Bioplastic	Bio-Monomer
Polylactic Acid (PLA)	D,L-lactic acids
Poly(butylene succinate) (PBS)	succinic acid, 1,4-butanediol
Poly(trimethylene terephthalate) (PTT)	1,3-propanediol
Polyethylene (PE)	bioethylene
Polypropylene (PP)	bioisobutanol
Polyethylene Terephthalate (PET)	bioethylene glycol
Poly(propylene carbonate) (PPC)	carbon dioxide

The physical properties of each polymer differ, making it not all suitable for lost foam casting as the material property that makes polystyrene castable using the lost foam casting process is unknown. The bond energy density of the polymer molecule is hypothesized to be what determines if a polymer is castable using lost foam (Figure 2). Bieniewicz et al. developed a low thermal degradation hot melt adhesive that increased the metal front velocity by reducing the energy density of the polymer.[11]

During casting, energy from the metal front is exothermically transferred to the foam pattern to expend it. A pattern material requiring minimal energy to vaporize/sublimate per unit volume would have the best chance of filling without defects like misruns. However, this is not the only controlling physical property as other factors that influence castability include decomposition temperature range, volume of gases from polymer decomposition, and bead fusion.

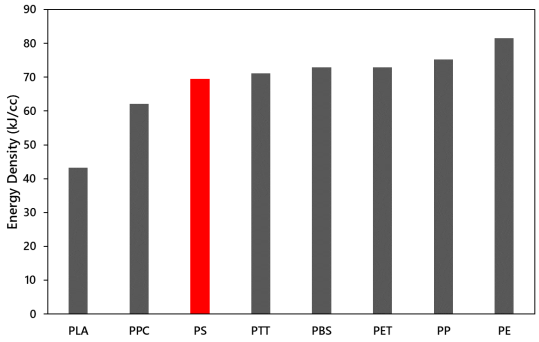

Figure 2. The energy density of bio-based polymers (gray) compared to polystyrene (red) based on the bond energies within the molecules.

The heavy dependency modern society has on crude oil for the manufacturing of plastic products (polystyrene) creates a disadvantage for future generations. The National Society of Professional Engineers (NSPE) encourages engineers to adhere to the principles of sustainable development to protect the environment for future generations.[12] When the world's oil reserves are exhausted, humanity will quickly need to find alternatives to produce plastics and other petroleum products. If no alternatives are found in time, the lost foam casting processes will cease to exist. To help ensure the long-term sustainability of the lost foam casting process, this research aimed to identify an environmentally sustainable alternative to the current petroleum derived polystyrene.

MATERIALS AND METHODS

FOAM MOLDING

Biofoam molding, particularly using expanded polylactic acid (EPLA), has emerged as a promising alternative in lost foam applications. Research has explored various EPLA formulations, each offering different performance characteristics. The formulations tested (Figure 3) represent a select range of EPLA compositions, each tailored for specific applications. Bioffex 412 (EPLA 4) has better leak resistance and bead-to-bead sintering possibly translating into reduced porosity of lost foam patterns. Bioffex 303 (EPLA 3) has enhanced heat resistance and better insulation equating to better dimensional stability and reduced shrinkage. Bioffex 211 (EPLA 2) has less than 1% additives while maintaining a low density and ease of processing.

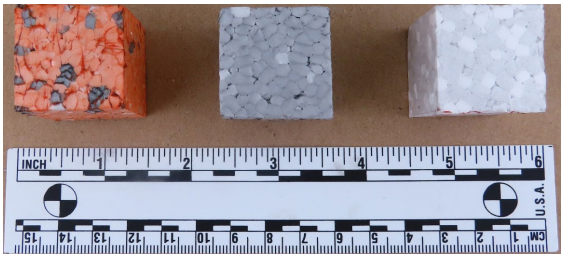

Figure 3. One inch cube samples used for material characterization. From left to right: EPLA 4, 3, and 2.

EPS foam patterns were molded at ATLAS Molded Products (Fond du Lac, WI) and the EPLA foam patterns were molded at LifeFoam Industries (Greer, SC) using a Kurtz K68 shape molding machine outfitted with a single cavity tool featuring a specific sprue shape and a core-pull mechanism for part extraction to produce the hollow-core part (Figure 4). The EPLA foam patterns for the casting trial were produced using EPLA 2 with a density of 1.5 pounds per cubic foot (pcf). While other formulations incorporate different additives to enhance thermal resistance, expansion characteristics, and fusion properties, EPLA 2 was chosen as a near-baseline EPLA formulation to gain a more fundamental understanding of EPLA performance in lost foam applications. Fifteen test objects were produced for each casting trial in aluminum and cast iron (Figure 5).

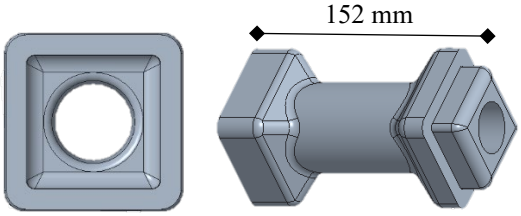

Figure 4. Schematic of test object.

The tooling was configured to optimize the molding of EPLA bead foam, considering factors such as reduced heat resistance and material shrinkage. The EPLA molding process utilized a modified steam chest shape-molding process to address the unique challenges of EPLA foams, particularly the lower heat resistance when compared to traditional EPS. Additionally, EPLA does not utilize hydrocarbon blowing agents, which can be responsible for residual explosive gases in foam, allowing for the molding process to operate at a significantly lower temperature range, 185-212F (85-100C), compared to conventional EPS molding temperatures 212-230F (100-110C).

The molding cycle consisted of several key steps: filling, steaming, vacuum stabilization, cooling, and ejection. Foam particles were introduced into the cavity under pressure through a single fill gun. After the cavity was filled, steam was gradually applied to the steam chest, increasing pressure in the mold up to 0.3 bar (4.4 psi). Once the target pressure was reached, the steam was turned off and the steam chest was exposed to vacuum generated by a liquid ring vacuum pump. The vacuum stabilization phase, lasting only a few seconds, ensured the removal of positive pressure and residual water on the part.

Foam pattern permeabilities of the EPS and EPLA were tested with a vacuum pattern permeability apparatus.[13] Four separate locations around the pattern with four replicates each were used to establish the pattern permeability.

Figure 5. Molded test object (Figure 4) patterns in EPS (left) and EPLA (right).

THERMOGRAVIMETRIC ANALYSIS (TGA)

Thermogravimetric analysis (TGA) was used to study the differences in decomposition behavior between EPLA and EPS. A 3.773±0.258 mg sample of each foam was tested using a TA Instruments Discovery TGA 550 with an inert nitrogen atmosphere. Samples were heated at a constant rate of 36 F/min (20 C/min) up to 1382F (750C) ensuring complete decomposition.

DIFFERENTIAL SCANNING CALORIMETRY (DSC)

Differential scanning calorimetry (DSC) was used to measure temperatures and heat flows associated with thermal transitions in the EPLA and EPS. A 1.200±0.100 mg sample of each foam was tested using a TA Instruments Discovery DSC 250 with an inert nitrogen atmosphere. Samples were heated at a constant rate of 18 F/min (10 C/min) to 527F (275C), cooled at a constant rate of 18 F/min (10 C/min) to 32F (0C), then heated again at a constant rate of 18 F/min (10 C/min) to 527F (275C).

PYROLYSIS GAS CHROMATOGRAPHY-MASS SPECTROMETRY (GC-MS)

Duplicate specimens from each sample were prepared for pyrolysis GC-MS by cutting a portion off a single foam bead with a cleaned razor blade to yield a mass of approximately 100 µg. A CDS 6200 Pyroprobe with

autosampler was used, with nitrogen as the pyrolysis gas. Samples were heated to 1472F (800C) for 15 seconds. Analysis was performed using an Agilent 6890 Gas Chromatograph coupled with an Agilent 5973 Mass Spectrometer. The injection temperature was 572F (300C), with hydrogen as the carrier gas at a flow rate of 0.7 mL/min. Detection was set to scan mode (m/z 36-600). Peak identification was performed using the 2023 NIST/EPA/NIH mass spectral library, NIST Mass Spectral Search Program (v2.3), AMDIS (v2.73), and the CDS polymer pyrolysis and additive library.

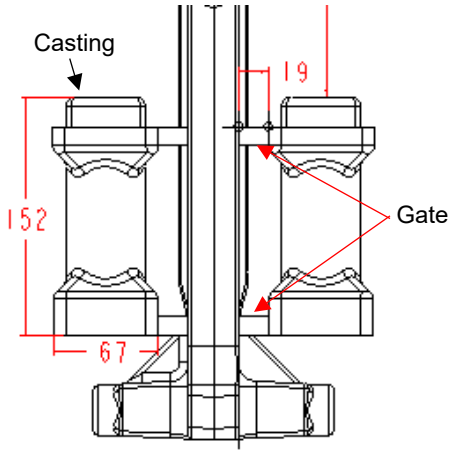

Figure 6. Vertical casting orientation with an EPLA pattern (left) and EPS (right). The castings are bottom filled with a gate at the bottom and top of the casting. Dimensions in red (mm).

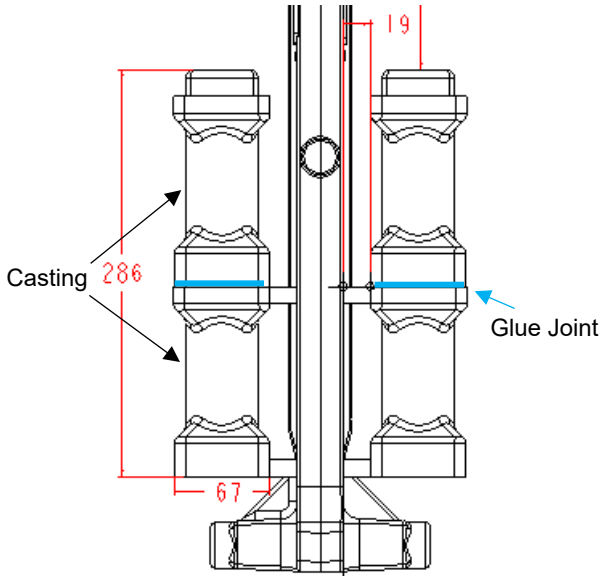

Figure 7. Vertical casting orientation with two patterns glued on top one another with EPLA pattern (left) and EPS (right). Castings are bottom filled with same gating as Figure 6 for the bottom casting only. Dimensions in red (mm).

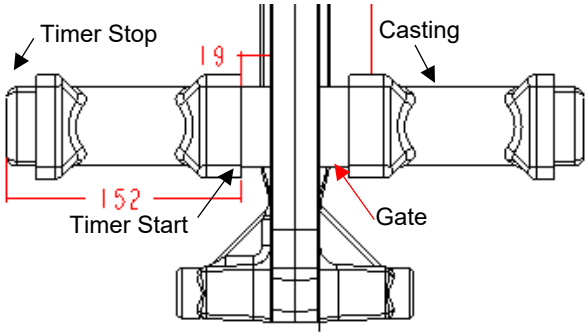

Figure 8. Horizontal casting orientation with EPLA pattern (left) and EPS (right). The castings are side filled. Dimensions in red (mm).

CASTING

The EPS and EPLA patterns (Figure 4) were glued to EPS gating systems in three orientations (Figs. 6-8) with four replicates per orientation. The castings were poured in both aluminum and gray cast iron. To measure the difference in aluminum metal front velocities between the two materials during filling, thermocouples were inserted into the bottom and top of the foam patterns (Figure 8) to make a timer circuit.

Temperature was measured using an Arduino Uno R3 with MAX31855 cold-junction compensated thermocouple-to-digital converters and recorded using CoolTerm version 2.2.0. As the metal front contacted the first thermocouple and the temperature rose above 122F (50C), the timer started and stopped when the metal contacted the second thermocouple, and it rose above 122F (50C) (See Appendix).[11] Only one replica was tested due to a constraint in the number of patterns available.

Aluminum

The aluminum casting trials were completed at Mercury Marine (Fond du Lac, WI). Foam pattern assemblies (Figs. 6- 8) were dip coated using ASK CERAMCOTE EP9 AL MERC with a perm of 8.8. Patterns were dried at 115 ± 5F (46 ± 3C) for 72 hours before compaction in Carbo Ceramics ID-40 synthetic mullite.

Alloy A356 was melted in a dry hearth furnace, filtered with a ceramic filter furnace, degassed with N_2 using a rotary degasser, and additions of Al-10%Sr and Al-5%Ti-1%B wire were injected for eutectic modification and grain refinement before being poured at 1450 ± 15F (787 ± 8C) using a robotic ladling system (Figure 9). The molds cooled for an hour before the castings were extracted and degated. Castings were shotblasted before being x-rayed for porosity/inclusions and measured using a laser scanner.

Figure 9. The robotic pouring system at Mercury Marine (Fond du Lac, WI). (Image courtesy of Mercury Marine.)

Gray Cast Iron

The gray cast iron casting trials were completed at Betz Industries (Grand Rapids, MI). Foam patterns were dipped using Refcotec Refcobar 6010TN with a permeability of 16. Patterns were dried at 100F (38C) for 4 hours before casting. The patterns were then attached to a cellulose gating system (Figs 6-8) with the upper ingate removed before being compacted in silica sand with a grain fineness number (GFN) of 37. ASTM A48 CL40 was melted in a 20-ton coreless induction furnace. The iron was inoculated with a barium containing inoculant. The molds were then hand poured at 2599F (1426C). After one hour, the castings were removed from the mold and shotblasted. The castings were then degated and measured with a laser scanner.

RESULTS

THERMAL ANALYSIS

The TGA and DSC results for EPS and the three EPLA foams are displayed in Table 2. The objective is to have the EPLA foams decompose at the same or lower temperatures of the EPS baseline. The EPLAs did not completely decompose, resulting in a small amount of residue compared to the EPS.

Table 2. Thermal Analysis Results from TGA and DSC

Material	Onset Decomposition Temperature (C)	Onset Melting Temperature (C)	% Residue
EPS	391	250	0.17
EPLA 4	336	142	1.19
EPLA 3	319	141	1.63
EPLA 2	338	116	1.07

PYROLYSIS GC-MS

The degradation of EPS produced over 75 identifiable degradants with the major products being styrene, toluene, bibenzyl, methyl styrene, ethyl benzene, indene, and naphthalene. The most significant group was styrene and its derivatives, comprising approximately 73% of the total composition, with styrene itself accounting for 70%. Toluene was the next most abundant compound, making up approximately 5%. Naphthalene and its derivatives constituted about 4% of the composition, while indene and its derivatives were present at around 3%. Stilbene and its derivatives accounted for approximately 2% of the total. Benzene and its derivatives made up roughly 1%. The remaining 12% consisted of various other compounds, including phenanthrene, fluorene, biphenyl, anthracene, and others. These groupings are based on the structural similarities of the detected compounds and may include various isomers and derivatives of the primary named compounds.

The degradation of the EPLA produced 15 major identifiable degradants being lactide, 2-butanone, glycidol, 1,4-cyclohexadiene, 1,3-cyclopentadiene, and 2-methyl-propanal. The most significant group was lactide and related compounds comprising approximately 35% of the total composition. The next grouping was based on the presence of a ketone functional group and accounted for 27% of the total composition. Glycidol and related compounds accounted for 17% of the total composition. Cyclopentadienes and cyclohexadienes accounted for 8% of the total composition. Chemicals which contained a furan ring structure accounted for 5% of the total composition. Lastly, other compounds accounted for 8% of the total composition. These groupings are based on the structural similarities of the detected compounds and may include various isomers and derivatives of the primary named compounds. The EPLA degradants consisted of lower molecular weight materials compared to EPS degradants (Table 3).

Table 3. Distribution of Degradants Molecular Weights from EPS and EPLA

Molecular Weight (Daltons)	EPS	EPLA
<100	6%	64%
100-144	78%	36%
144-265	15%	0%

FOAM PERMEABILITY

The molded foam permeabilities for EPS and the EPLA are shown in Table 4. The large bead size of the EPLA resulted in a higher perm that exceeds the 125 ml/min limit set by Barendreght and Littleton[14] to avoid turbulent filling.

Table 4. Foam Permeability Measurements with 95% Standard Deviation of the Mean

Material	Permeability (ml/min)
EPS	32±0
EPLA	141±6

CASTING QUALITY AND METROLOGY

Images of the cast test pieces are shown in Figure 10-Figure 12 for aluminum and Figure 13-Figure 15 for gray iron. The aluminum castings filled out perfectly with no visual defects regardless of the pattern material. The rough surface finish from the large bead size of the EPLA is clearly visible. The vertically cast gray iron casting match the casting quality of the aluminum, but the double stacked (Figure 14) and horizontal (Figure 15) castings show incomplete filling of the casting.

Figure 10. Image of vertically cast aluminum parts. EPS (left) and EPLA (right).

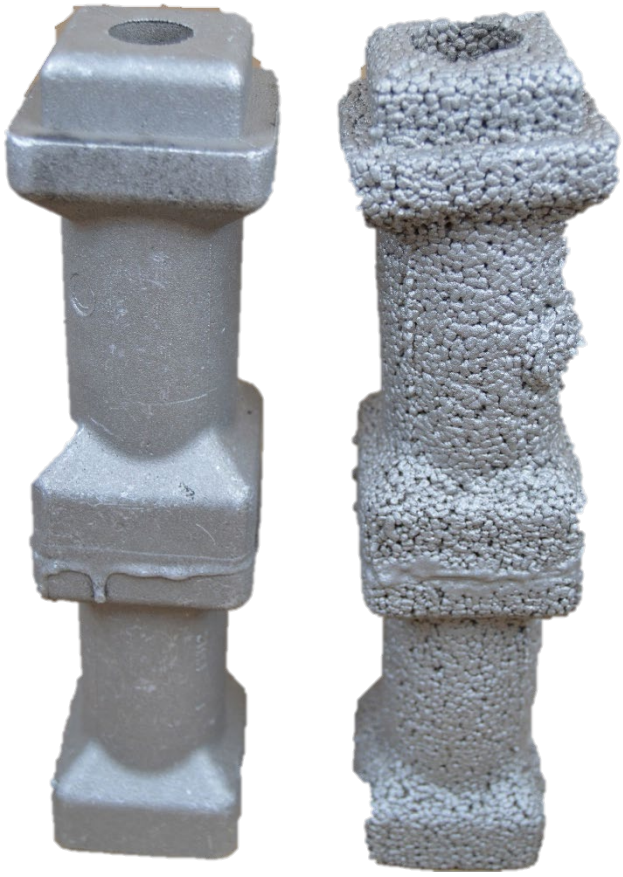

Figure 11. Image of vertically cast aluminum parts vertical casting orientation with two patterns glued on top one another. EPS (left) and EPLA (right).

Figure 12. Image of horizontally cast aluminum parts. EPS (left) and EPLA (right).

Figure 13. Image of vertically cast gray iron parts. EPS (right) and EPLA (left).

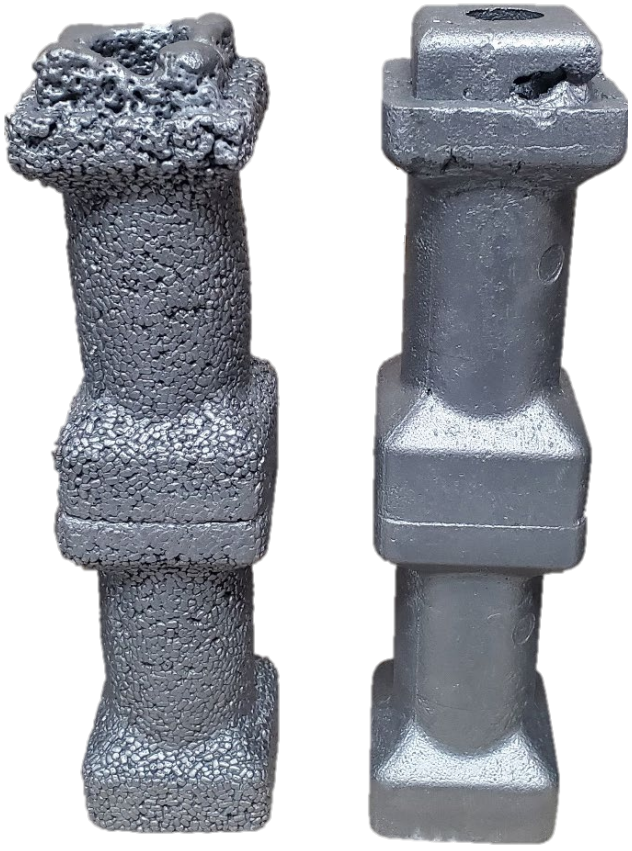

Figure 14. Image of vertically cast gray iron parts vertical casting orientation with two patterns glued on top one another. EPS (right) and EPLA (left).

Figure 15. Image of horizontally cast gray iron parts. EPS (right) and EPLA (left).

X-ray images of the aluminum castings (Figs. 16-17) are compared between the different pattern material and casting orientations. Sectioned aluminum castings (Figure 18) show the EPLA's large inter-bead voids allowed for coating to penetrate and become entrained in the casting.

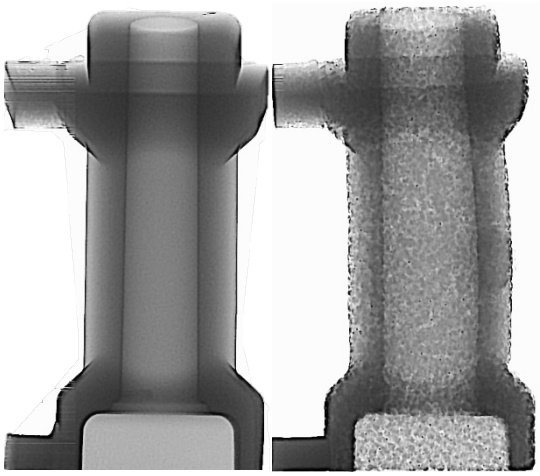

Figure 16. An X-ray image of vertically cast aluminum parts with ingates facing left. EPS (left) and EPLA (right).

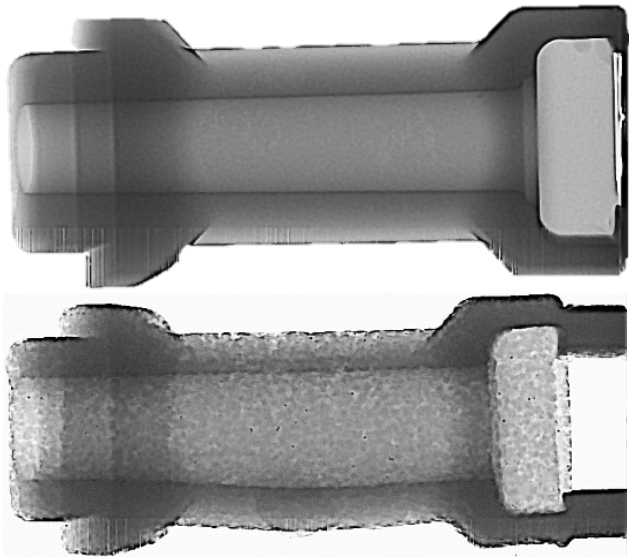

Figure 17. An X-ray image of horizontally cast aluminum parts. EPS (top) and EPLA (bottom).

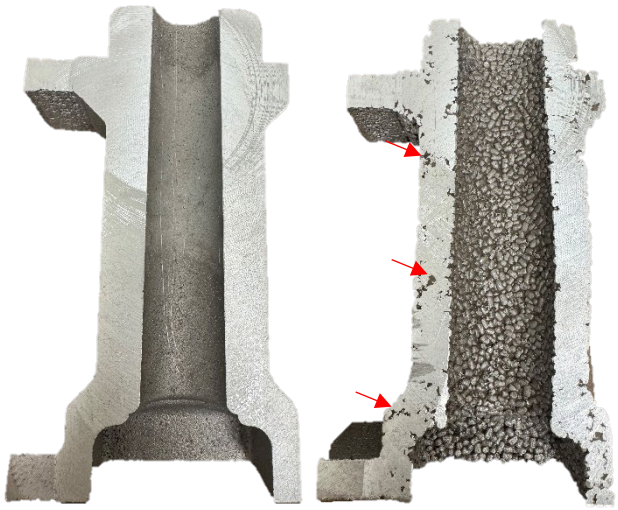

Figure 18. Sectioned aluminum castings. The EPS (left) is free of any visual defects where EPLA (right) has entrained coating (red arrow).

Results from the melt front velocity trial are shown in Table 5. The aluminum melt front traveled slowest through the EPS pattern with the EPLA evaporating 14% faster.

Table 5. Melt Front Velocities for EPS and EPLA

Material	Melt Front Velocity (mm/sec)
EPS	29.54
EPLA	33.56

Laser scans of the aluminum (Figs. 19-20) and gray iron (Figs. 21-22) castings are compared between the different pattern materials. Gating remained on the castings during scanning as an alignment feature to merge the two scans and get all the surfaces. Scans were aligned with a best fit to the model.

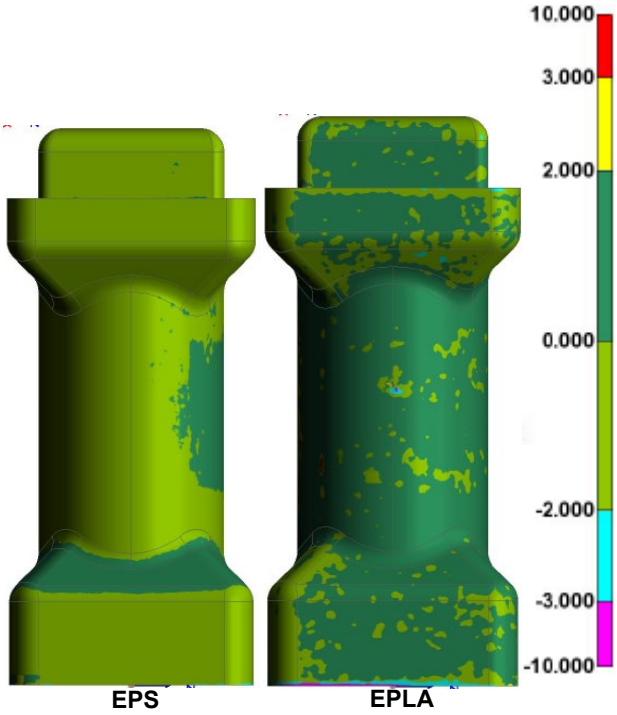

Figure 19. Laser scan of vertical orientation of the aluminum casting from EPS (left) and EPLA (right). Scale bar is in mm.

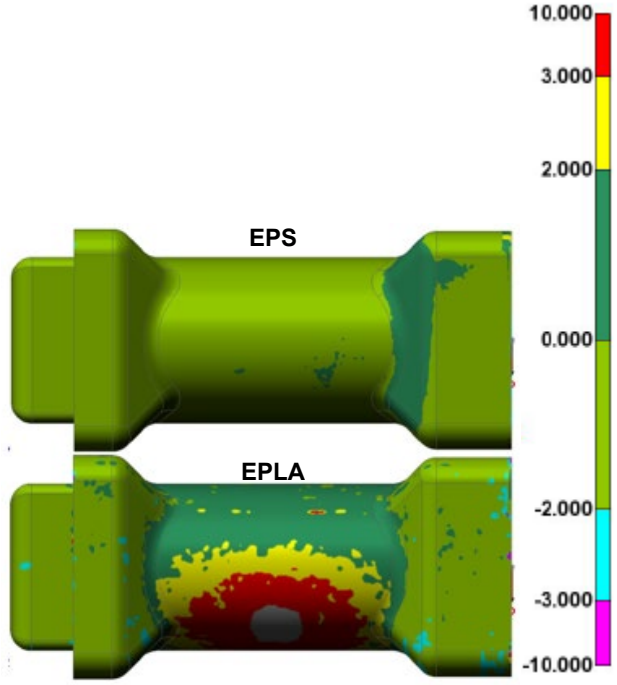

Figure 20. Laser scan of horizontal orientation of the aluminum casting from EPS (top) and EPLA (bottom). Scale bar is in mm.

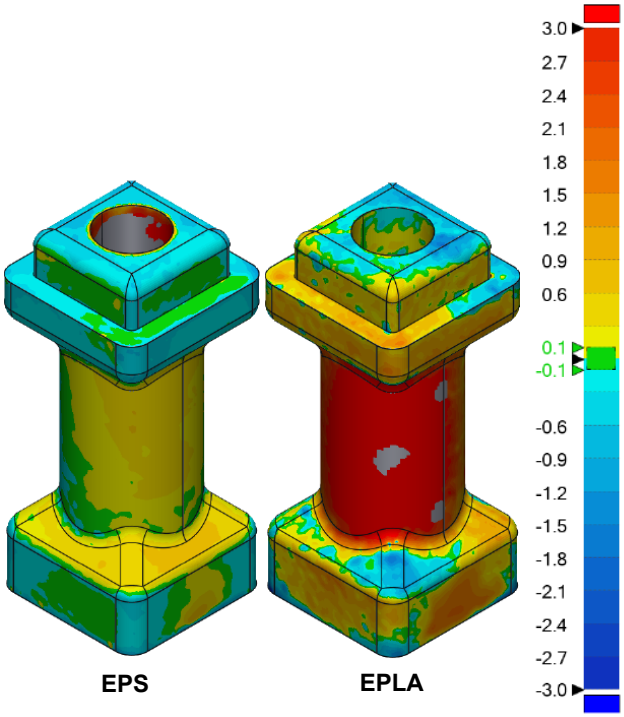

Figure 21. Laser scan of vertical orientation the gray iron casting from EPS (left) and EPLA (right). Scale bar is in mm.

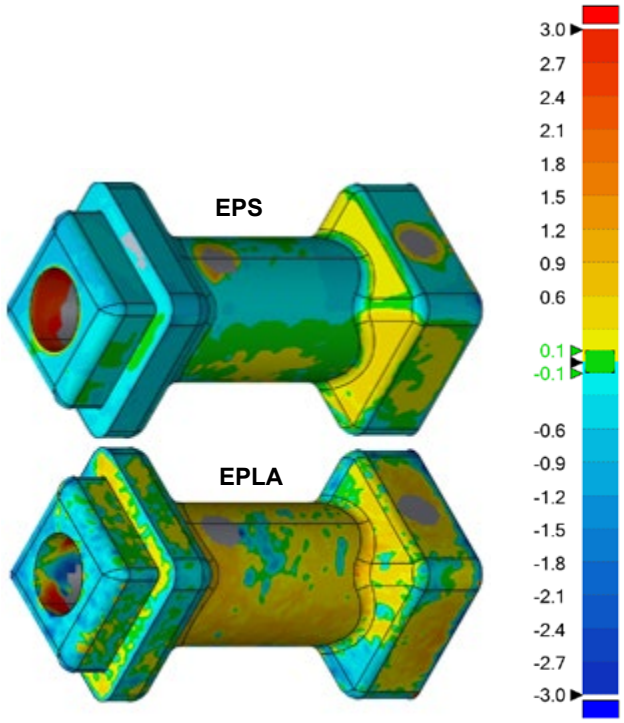

Figure 22. Laser scan of the horizontal orientation of gray iron casting from EPS (top) and EPLA (bottom). Scale bar is in mm.

DISCUSSION

MATERIAL PROPERTIES

Preliminary assessment of the energy density hypothesis via thermal degradation curves agreed with expectations (Table 2). The EPLA had a lower thermal degradation temperature and melting point than the EPS foam, which was expected given its lower energy density (Figure 2). The EPS fully degraded (>99.8%) where the EPLA had 1-1.5 % residue which could become entrapped in the metal front and result in inclusions. The higher residue is likely due to the EPLA degradants containing oxygen which lowers their volatility. Furthermore, the EPLA degradants containing oxygen have a lower fuel value opposite degradants produced by EPS.

The results of the GC-MS showed a difference in the emissions expected between EPS and the EPLA. Section 112 of the Clean Air Act, EPA (1970)[15] designates styrene, toluene, ethyl benzene, and naphthalene as HAPs meaning emissions controls, such as VOC thermal oxidizers, are required if emissions exceed 10 tons/year. None of the EPLA degradants measured are classified as HAPs by the EPA meaning emissions controls are only required if emissions were to exceed the 25 tons/year federal threshold.[15] Local and individual state regulations at a minimum must include the same federally designated 188 HAPs but could include additional chemicals and lower emission thresholds.

Many of the EPS degradants (styrene, toluene, benzene, etc.) are reasonably anticipated to be human carcinogens further warranting emissions controls.[16] However, pyrolysis GC-MS showed that there were no hazardous aryl molecules (e.g., styrene, benzene derivatives, etc.) produced with the pyrolysis of EPLA. Glycidol is the only degradant reasonably anticipated to be a human carcinogen from the EPLA although no epidemiological studies have been identified that evaluated the relationship between human cancer and exposure specifically to glycidol.[16]

The degradation products from EPLA vaporize more readily and completely, leading to a faster, more efficient burning process that occurs at lower temperatures compared to EPS. The lower molecular weight degradants of EPLA (Table 3) will flash off easier during casting, while the higher molecular weight degradants seen in EPS will remain deposited in sand and require burn-off to be removed.

The consistent use of a near-baseline formulation across all tests, including TGA and GC-MS analyses, ensures direct comparability of results and provides a clear foundation for understanding the fundamental behavior of EPLA in lost foam casting applications.

CASTING QUALITY

The level of casting quality produced from this trial supports the future use of EPLA foam patterns as an alternative to traditional EPS patterns given the bead size can be reduced to modern lost foam pattern "T" bead size. The EPLA 2 bead, having no additives, was successful in producing sound aluminum castings regardless of the casting orientation. If the EPLA bead size were the same as the EPS, it would be safe to conclude the castings would be indistinguishable from a casting quality and processing view as the EPLA was produced, without issue, using the same process technology and parameters as the EPS patterns. The same conclusion cannot be made for the gray iron castings. All the gray iron molds blew back from the decomposition gasses leading to interrupted pouring and poor filling (Figs. 14-15). Ferrous lost foam casters typically use a co-polymer blend, such as PMMA, that helps slow the metal front down to allow for a laminar filling and thus avoiding the dangerous gas-metal blow back event. The EPLA 3 or 4 formulations might provide a similar aiding affect, but further trials are required. The horizontally cast samples had mold collapse for both the EPS and EPLA, although the EPLA more so. Mold collapse could have resulted from poor compaction, but most likely a result of the interrupted pouring causing a loss of kinetic zone pressure.[17]

The x-ray results for the EPS patterns showed porosity free castings for both horizontal and vertical orientations (Figs. 16-17). The EPLA castings are difficult to judge porosity as the large bead gaps on the surface show the same as internal porosity would. Castings were sectioned (Figure 18) to investigate the potential of sub-surface porosity and found that the EPS patterns were defect free as indicated by x-ray, but the EPLA contained voids that were filled with coating. This indicates the large inter-bead voids of the EPLA allowed the coating to penetrate during dipping and become entrained in the casting. Further reducing the bead size will alleviate this issue. Another noticeable difference between the EPS and EPLA was the consistency of the internal core. The EPS castings maintained a straight walled core regardless of the casting orientation while the EPLA has a bow on one side of the casting. The deformation likely occurred during the molding process as both orientations have the same curvature given different sand compaction and filling between the two sample orientations.

The metal front velocities for the different pattern materials gave an unexpected result for the EPLA. Aluminum is generally known to move through a well fused EPS pattern around 25mm/sec (1 in/sec) which matches the measured velocity (Table 5). The EPLA pattern given its high permeability, roughly 4.5 time higher than EPS (Table 4), was expected to have a melt front velocity representative of the difference in permeabilities. One possible explanation for the slower than expected metal velocity could be the EPLA produced more gas resulting in a higher system back pressure, slowing the metal front down.

The 3D scans of the castings show discrepancies between the EPLA and EPS patterns for both aluminum and gray iron (Figs. 19-22). The EPS patterns cast in aluminum aligned with the model perfectly regardless of orientation (Figs. 19-20) as expected given the model was designed for aluminum-EPS. The aluminum-EPLA patterns performed well dimensionally in the vertical orientation (Figure 19) but show large amounts of positive variance in the horizontal orientation (Figure 20). The casting profile deviation is from the fill gun in the molding tool (Figure 10) and not a result of the casting orientation. The gray iron scans showed the same trend as the aluminum casting result with the EPS patterns having greater dimensional accuracy (Figs. 21-22). The positive material condition on the vertical EPLA casting (Figure 21) is the same fill gun area as the horizontal aluminum casting. Overall, the gray iron castings conformed to the model accurately given the differences in thermal expansion between aluminum and gray iron.

CONCLUSION

Historically, the lost foam casting process has used EPS for the pattern material, but a novel molding bead technology has emerged that derives an EPLA molding bead from sustainable domestic biological sources. Bio-based foam patterns were evaluated for their potential to replace EPS as a lost foam pattern material using laboratory testing and casting trials. TGA showed the EPLA decomposed at lower temperatures than EPS, but not to completion. The GC-MS confirmed the EPLA materials do not produce HAPs or carcinogens, making the material safer for foundries. The casting trials successfully produced sound lost foam castings using aluminum and with some challenges using gray cast iron without any modifications to the lost foam casting process.

ACKNOWLEDGMENTS

This research was funded by the American Foundry Society (22-23#04) sponsored by the Lost Foam Division with in-kind contributions from Mercury Marine, Betz Industries, ATLAS Molded Products, and Lifoam Industries.

REFERENCES

1. Hazardous Substance Research Centers/South and Southwest Outreach Program, "*Environmental Impact of the Petroleum Industry*" Environmental Update #12, (June 2003).

https://cfpub.epa.gov/ncer_abstracts/index.cfm/fuseaction/display.files/fileID/14522. (Link last accessed 01-08-2025.)
2. Alexander Martin, "Environmental Fate and Effects of Styrene," *Critical Reviews in Environmental Science and Technology*, 27(4):383-410 (Oct. 1997). https://doi.org/10.1080/10643389709388504 (Link last accessed 01-08-2025.)
3. Fractional Distillation. Available at: https://www.studysmarter.us/explanations/chemistry/organic-chemistry/fractional-distillation/ (Link last accessed October 19, 2022.)
4. "Oil left in the world," *worldometer* (2016). https://www.worldometers.info/oil/#:~:text=World%20Oil%20Reserves&text=The%20world%20has%20proven%20reserves,levels%20and%20excluding%20unproven%20reserves). (Link last accessed 01-08-2025.)
5. "Proved Reserves of Crude Oil and Natural Gas in the United States, Year-End 2020," U.S. Energy Information Administration (EIA), Washington, DC (2022). https://www.eia.gov/naturalgas/crudeoilreserves/ (Link last accessed 01-08-2025.)
6. Bates, Charles, Personal communication.
7. "Energy and Environmental Profile of the U.S. Metalcasting Industry," Prepared by Energetics, Incorporated for the U.S. Dept. of Energy, Office of Industrial Technologies, Columbia, Maryland (Sept. 1999). https://www.energy.gov/eere/amo/articles/itp-metal-casting-energy-and-environmental-profile-us-metal-casting-industry (Link last accessed 01-08-2025.)
8. "Literature Review and Analysis of EPC Emissions and Solid Waste Generation," American Foundrymen's Society, *Research Report* (June1991).
9. Shroyer, H.F., Inventor, "Cavityless Casting Mold and Method of Making Same, U.S. Patent #2,830,343, Filed April 15, 1956.
10. Guler, K.A., Karaaslan, A, Kisasöz, A., "A study of expanded polyethylene (EPE) pattern application in aluminium lost foam casting," *Russian Journal of Non-Ferrous Metals*, (April 2015);56(2):171-176.
11. Bieniewicz, K., Reich, M., Soraruf, N., Steer, A., Sanders, P., Belke, J., "Improving Metal Flow in Lost Foam Casting Through Use of Low Thermal Degradation Hot Melt Adhesives," *Inter Metalcast,* (April 2024). https://doi.org/10.1007/s40962-024-01331-7 (Link last accessed 01-08-2025.)
12. "NSPE Code of Ethics for Engineers," National Society of Professional Engineers. Code of Ethics (July 2019). https://www.nspe.org/sites/default/files/resources/pdfs/Ethics/CodeofEthics/NSPECodeofEthicsforEngineers.pdf. (Link last accessed 01-08-2025.)
13. Littleton, H.E., Molibog, T., Sun, W., "The Role of Pattern Permeability in Lost Foam Casting, *Transactions of the American Foundry Society,* pp.1265-1277 (2003).
14. Barendreght, J.A., Littleton, H.E,. "Development and Validation of a Lost Foam Pattern Quality Measurement System," *Transactions of the American Foundry Society*, pp. 923-937 (2007).
15. Clean Air Act, §7401 et seq., 42 U.S.C., (1970).
16. "Report on Carcinogens," Fifteenth Edition, NTP (National Toxicology Program), Research Triangle Park, NC: U.S. Department of Health and Human Services (2021).
17. Allen, K.R., Belke, J.A., "Loss of Kinetic Zone Pressure Causes Mold Wall Collapse During Filling Across a Glue Joint in Lost Foam Casting," *IJMC/FEF Student Research Competition. Inter Metalcast* **18**, 23–29 (2024). https://doi.org/10.1007/s40962-023-01185-5 (Link last accessed 01-08-2025.)

APPENDIX

```
#include <SPI.h>
#include <Adafruit_MAX31855.h>

// Define pins for thermocouples
#define TC1_CLK 5
#define TC1_CS 6
#define TC1_DO 7
#define TC2_CLK 11
#define TC2_CS 12
#define TC2_DO 13

// Constants
#define THRESHOLD_TEMP 50.0  // Temperature threshold in °C
#define DISTANCE 152.0       // Distance between thermocouples in mm

// Create thermocouple objects
Adafruit_MAX31855 thermocouple1(TC1_CLK, TC1_CS, TC1_DO);
Adafruit_MAX31855 thermocouple2(TC2_CLK, TC2_CS, TC2_DO);

bool tc1_triggered = false;
bool tc2_triggered = false;
unsigned long startTime = 0;
unsigned long endTime = 0;

void setup() {
  Serial.begin(9600);
  delay(2000);  // Wait for MAX31855 to stabilize
  Serial.println("Starting melt front velocity measurement...");
}

void loop() {
```

```
  double temp1 = thermocouple1.readCelsius();
  double temp2 = thermocouple2.readCelsius();

  // Check if the first thermocouple is triggered
  if (temp1 > THRESHOLD_TEMP && !tc1_triggered) {
    tc1_triggered = true;
    startTime = millis();
    Serial.print("TC1 triggered at ");
    Serial.print(temp1);
    Serial.println(" °C");
  }

  // Check if the second thermocouple is triggered
  if (temp2 > THRESHOLD_TEMP && tc1_triggered
&& !tc2_triggered) {
    tc2_triggered = true;
    endTime = millis();
    Serial.print("TC2 triggered at ");
    Serial.print(temp2);
    Serial.println(" °C");

    // Calculate time difference and velocity
    unsigned long timeElapsed = endTime - startTime;
    double velocity = (DISTANCE / timeElapsed) * 1000;
// Convert to mm/sec

    // Output the results
    Serial.print("Time to move between TC1 and TC2: ");
    Serial.print(timeElapsed);
    Serial.println(" ms");
    Serial.print("Melt front velocity: ");
    Serial.print(velocity);
    Serial.println(" mm/sec");
  }
}
```